algorithms

MDPI

Article

A Mathematical Study on a Fractional-Order SEIR Mpox Model: Analysis and Vaccination Influence

Iqbal M. Batiha [1,2], Ahmad A. Abubaker [3,*], Iqbal H. Jebril [1], Suha B. Al-Shaikh [3], Khaled Matarneh [3] and Manal Almuzini [4,5]

[1] Department of Mathematics, Al Zaytoonah University, Amman 11733, Jordan; i.batiha@zuj.edu.jo (I.M.B.); i.jebril@zuj.edu.jo (I.H.J.)
[2] Nonlinear Dynamics Research Center (NDRC), Ajman University, Ajman 346, United Arab Emirates
[3] Faculty of Computer Studies, Arab Open University, Riyadh 11681, Saudi Arabia; s.alshaikh@arabou.edu.sa (S.B.A.-S.); k.matarneh@arabou.edu.sa (K.M.)
[4] School of Mathematical Sciences, Universiti Sains Malaysia, Penang 11800, Malaysia; almuzini2023@student.usm.my
[5] Department of Mathematics and Statistics, American University of Sharjah, Sharjah 26666, United Arab Emirates
* Correspondence: a.abubaker@arabou.edu.sa

Abstract: This paper establishes a novel fractional-order version of a recently expanded form of the Susceptible-Exposed-Infectious-Recovery (SEIR) Mpox model. This model is investigated by means of demonstrating some significant findings connected with the stability analysis and the vaccination impact, as well. In particular, we analyze the fractional-order Mpox model in terms of its invariant region, boundedness of solution, equilibria, basic reproductive number, and its elasticity. In accordance with an effective vaccine, we study the progression and dynamics of the Mpox disease in compliance with various scenarios of the vaccination ratio through the proposed fractional-order Mpox model. Accordingly, several numerical findings of the proposed model are depicted with the use of two numerical methods; the Fractional Euler Method (FEM) and Modified Fractional Euler Method (MFEM). Such findings demonstrate the influence of the fractional-order values coupled with the vaccination rate on the dynamics of the established disease model.

Keywords: Mpox model; Caputo fractional-order operator; SEIR model; stability; basic reproductive number; elasticity indices

Citation: Batiha, I.M.; Abubaker, A.A.; Jebril, I.H.; Al-Shaikh, S.B.; Matarneh, K.; Almuzini, M. A Mathematical Study on a Fractional-Order SEIR Mpox Model: Analysis and Vaccination Influence. *Algorithms* **2023**, *16*, 418. https://doi.org/10.3390/a16090418

Academic Editor: Alicia Cordero

Received: 24 July 2023
Revised: 29 August 2023
Accepted: 30 August 2023
Published: 1 September 2023

1. Introduction

Mathematical modeling has turned into an invaluable tool in revealing the behaviors of infectious diseases and formulating effective control strategies. Mpox, a viral disease with similarities to smallpox, has attracted considerable attention in the field of epidemiological models due to its potential impact on human health. As the Mpox disease is a viral zoonotic infection, it might transmit from animals to people. In addition, it might transmit from the environment to a person, as it can transmit from one person to another [1]. In 2022, the Mpox disease began to spread like a pandemic in numerous countries all over the world. It is spreading now in some African countries [2,3].

To gain deeper insights into the transmission dynamics and develop accurate predictive models for Mpox, many researchers have increasingly explored the utilization of fractional calculus. Fractional calculus offers a promising tool for highlighting the intricate characteristics of infectious disease dynamics, as it allows for the incorporation of memory-dependent and non-local effects. Traditional models often suppose an instantaneous mixing by assuming that past interactions have no influence on future outcomes. So, from this point, the notion of fractional calculus might be utilized as an alternative to these models, as it can enable one to formulate a model of long-range dependence with extra freedom

of fractional-order values. This would enable a more realistic representation of the spread and evolution of the disease; see [4].

In the context of Mpox, fractional calculus can potentially enhance our understanding of various epidemiological factors such as transmission rates, recovery rates, and the impact of interventions. By incorporating fractional derivatives and integrals into the modeling framework, researchers can address the non-local nature of interactions and the presence of memory effects in disease transmission. These effects can reflect the persistence of immunity, delayed responses to interventions, or even other temporal dependencies; see [5]. Developing a fractional calculus-based model for Mpox involves considering fractional differential equations that can describe the growth of the diseased population over time. The fractional-order derivatives correspond to the memory or long-range dependence, which might be observed in the transmission of disease. Accurate estimation of the fractional-order value requires a combination of empirical evidence, fitting the model to available data, and a deep understanding of the underlying epidemiological processes [6]. The utilization of fractional calculus in modeling Mpox has the potential to yield valuable insights into the disease's dynamics and control strategies. Incorporating memory effects and non-local interactions in modeling the disease can provide a more accurate representation of its spread and evolution over time. Furthermore, such modeling can assist public health officials in evaluating and optimizing intervention strategies, estimating the impact of vaccination programs, and assessing the effectiveness of different control measures [7].

In this study, we aim to explore the application of fractional calculus in modeling Mpox transmission dynamics. By introducing fractional-order derivatives and considering memory-dependent effects, we attempt to enhance our understanding of the disease's behavior and provide valuable tools for policymakers and health care professionals in their efforts to mitigate and control Mpox outbreaks. For this purpose, a novel fractional-order version of the SEIR model is established in light of operating the Caputo operator. This model is analyzed with the help of proposing certain novel stability results, including the investigation of its invariant region, equilibria, Basic Reproductive Number (BRN), elasticity, and boundedness of solution, which is observed by using the Adomian decomposition method. Additionally, we also solved this model numerically using the Fractional Euler Method (FEM) and Modified Fractional Euler Method (MFEM) [8] for the aim of revealing the influence of the fractional-order values and the vaccination rate on the dynamics of the model at hand. In summary, this paper is arranged in the following manner. In the next part, some key definitions and basic concepts associated with fractional calculus are recalled briefly, whereas the formulation of the Mpox illness model is proposed in Section 3. In Section 4, we study the stability analysis of the Mpox model. In Section 5, we solve the proposed fractional-order Mpox model using the FEM and MFEM, followed by the conclusion of this work.

2. Preliminary Concepts

In this part, we recall fundamental descriptions and theorems related to fractional calculus, including the Riemann–Liouville integral and derivative, the Caputo derivative, and other relevant concepts [9].

Definition 1. *The Riemann–Liouville integral operator of the function* $h(x)$ *of fractional-order* $0 < \rho \leq 1$ *can be expressed by*

$$I^{\rho}h(x) = \frac{1}{\Gamma(\rho)} \int_0^x h(s)(x-s)^{\rho-1}\, ds, \quad x > 0. \tag{1}$$

In the following content, we list below some properties of the Riemann–Liouville integral operator:

$$I^{\rho}h(x) \to h(x) \text{ as } \rho \to 0, \tag{2}$$

$$I^{\rho}(x-a)^{\nu} = \frac{\Gamma(\nu+1)}{\Gamma(\rho+\nu+1)}(x-a)^{\rho+\nu}, \quad \nu \geq -1, a \in \mathbb{R}, \tag{3}$$

$$I^{\rho}I^{\lambda}h(x) = I^{\lambda}I^{\rho}h(x), \quad \rho, \lambda \geq 0, \tag{4}$$

$$I^{\rho}I^{\lambda}h(x) = I^{\rho+\lambda}h(x), \quad \rho, \lambda \geq 0. \tag{5}$$

Definition 2. *The Caputo fractional derivative operator of the function $h(x)$ of fractional-order $0 < \rho \leq 1$ can be expressed by*

$$^{C}D_{*}^{\rho}h(x) = \frac{1}{\Gamma(1-\rho)}\int_{0}^{x}\frac{h'(s)}{(x-s)^{\rho}}\,ds, \; x > 0. \tag{6}$$

Herein, we also list in what follows, some further properties of the Caputo derivative operator:

- For a constant c, we have $^{C}D_{*}^{\rho}c = 0$.
- For $a \in \mathbb{R}$, we have

$$^{C}D_{*}^{\rho}(x-a)^{\lambda} = \begin{cases} \frac{\Gamma(\lambda+1)}{\Gamma(\lambda-\rho+1)}(x-a)^{\lambda-\rho}, & \lambda > \rho-1, \\ 0, & \text{otherwise.} \end{cases}$$

- For constants a and b, $^{C}D_{*}^{\rho}$ is a linear operator, i.e.,

$$^{C}D_{*}^{\rho}(ah(x)+bg(x)) = a\,^{C}D_{*}^{\rho}h(x) + b\,^{C}D_{*}^{\rho}g(x).$$

In the same regard, it is important to remember the following basic property:

$$I^{\rho}\,^{C}D_{*}^{\rho}h(x) = h(x) - \sum_{k=1}^{n}h^{k}(0^{+})\frac{x^{k}}{k!}, \; x > 0, \tag{7}$$

where $n-1 < \rho \leq n$ such that $n \in \mathbb{N}$.

Definition 3. *The Caputo operator $^{C}D_{*}^{\rho}$ might be outlined in terms of the Riemann–Liouville integral operator along the following lines:*

$$^{C}D_{*}^{\rho}f = I^{n-\rho}D^{n}f, \tag{8}$$

where $\rho \in \mathbb{R}^{+}$ and $n = \lceil \rho \rceil$.

Definition 4 ([9])**.** *The two parameters of the Mittag-Leffler function can be expressed as*

$$E_{\gamma,\delta}(x) = \sum_{j=0}^{\infty}\frac{x^{k}}{\Gamma(\gamma k+\delta)},$$

where $\gamma, \delta > 0$ and $x \in \mathbb{C}$.

Theorem 1 ([9])**.** *Assume $^{C}D_{*}^{j\rho}h(x) \in C(0,T]$, for $j = 0, 1, 2, \cdots, n+1$ and $0 < \rho \leq 1$. Then, the function $h(x)$ might be expanded about x_0 in the following manner:*

$$h(x) = \sum_{j=0}^{n}\frac{(x-x_0)^{j\rho}}{\Gamma(j\rho+1)}(^{C}D_{*}^{j\rho}h)(x_0) + \frac{(x-x_0)^{(n+1)\rho}}{\Gamma((n+1)\rho+1)}(^{C}D_{*}^{(n+1)\rho}h)(\xi), \tag{9}$$

$\forall x \in (0,T]$, where $0 < \xi < x$.

3. Mpox Model

Mathematical models are extensively engaged in simulating the dynamics and the transmission of infectious diseases. In accordance with an effective vaccine, we study the progression and dynamics of the Mpox disease in compliance with various scenarios of the vaccination rate through a compartmental model of the type SEIR. In this paper, we consider the intervention of vaccination playing a significant role as a parameter, impacting on the model's dynamics. The equilibrium of the disease-free state will be determined, and then its stability with computing the BRN R_0^* will be examined in Section 4.

The diagram of the compartment model, including the vaccination rate for the aimed Mpox model, is shown in Figure 1, in which the total of the susceptible population is denoted by S, the total of the exposed population is denoted by E, the total of the infected population is denoted by I, and, finally, the total of the recovery population by R.

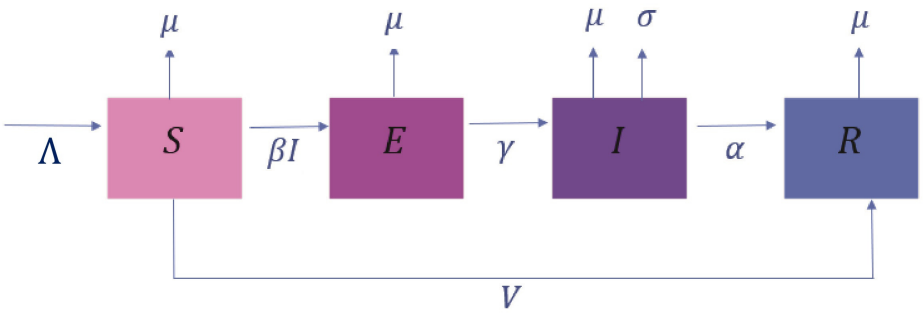

Figure 1. The compartment model, including vaccination rate.

In the same context, Figure 1 exhibits the parameters $(\Lambda, \sigma, \nu, \mu, \alpha, \gamma, \beta)$ that are responsible for the dynamics of the considered model. These parameters are outlined in Table 1.

Table 1. Model parameters.

Parameter	Denotation	Value
Λ	Rate of birth	Depending on country
γ	Rate of transmission (E to I)	$\left[\frac{1}{17}, \frac{1}{7}\right]$
β	Rate of transmission (S to E)	$[0.045, 0.18]$
α	Rate of transmission (I to R)	$\left[\frac{1}{32}, \frac{1}{15}\right]$
σ	Rate of fatality	$[0.03, 0.06]$
ν	Rate of vaccination	Variable $[0, 1]$
μ	Rate of natural death	Dependent on country

It is noteworthy that the rate of transmission β indicates the transmission's contact from S to E as a result of interacting with I cases. Additionally, γ^{-1} indicates the period of incubation, whereas α^{-1} indicates the period of recovery. In light of the aforementioned considerations, the conventional Mpox model might be described in the following manner [10]:

$$\begin{aligned} \frac{dS}{dt} &= \Lambda - \beta S(t)I(t) - (\nu + \mu)S(t) \\ \frac{dE}{dt} &= -(\mu + \gamma)E(t) + \beta S(t)I(t) \\ \frac{dI}{dt} &= \gamma E(t) - (\mu + \sigma + \alpha)I(t) \\ \frac{dR}{dt} &= \nu S(t) + \alpha I(t) - \mu R(t). \end{aligned} \tag{10}$$

with initial conditions

$$S(0) = S_0,\ E(0) = E_0,\ I(0) = I_0, R(0) = R_0. \tag{11}$$

For more clarification, model (10) is established in accordance with particular conditions, which might be stated as follows:

- The contact transmission parameter β does not take into account some factors, like climate, age, marital status, or gender.
- All of the model's parameters have no negative values.
- Inter-individual relations within society are distinguished by uniformity and homogeneity. This is because of the inherited suppositions for all of the model's states in which all persons have the same parameter value of the contact transmission regardless of their situations, such as their health circumstances or age.
- The size of population N is considered constant at any time, and it meets the following equality:
$$S(t) + E(t) + I(t) + R(t) = N(t). \tag{12}$$
- In the proposed model, the demography is taken into account, in which the natural death μ and natural birth Λ are incorporated.
- System (10) satisfies the following property:
$$\frac{dN}{dt} \leq h(N), \tag{13}$$
where h is a function depending only on N [11]. To see this, one can observe
$$\frac{dN}{dt} = \frac{d}{dt}(S(t) + E(t) + I(t) + R(t)) = \Lambda - \mu N - \sigma I.$$
Now, due to $\sigma I \geq 0$, we obtain
$$\frac{dN}{dt} \leq \Lambda - \mu N. \tag{14}$$
With the use of separation of variables, we can have
$$-(\Lambda - \mu N) \leq ce^t, \tag{15}$$
or
$$N \leq \frac{\Lambda}{\mu} + ce^t. \tag{16}$$
By using $N(0) = N_0$, we obtain
$$N(t) \leq \frac{\Lambda}{\mu} - \left(\frac{\Lambda}{\mu} - N_0\right)e^{-\mu t}. \tag{17}$$
Now, as $t \to \infty$, we obtain
$$N(t) \leq \frac{\Lambda}{\mu}, \tag{18}$$
and, hence, property (13) is held for system (10).

In order to propose the aimed fractional-order Mpox model, the Caputo operator ${}^{C}D_{*}^{\rho}$ is operated on the modified model (10) to obtain

$$\begin{aligned}
{}^{C}D_{*}^{\rho}S(t) &= \Lambda - \beta S(t)I(t) - (\nu + \mu)S(t)\\
{}^{C}D_{*}^{\rho}E(t) &= \beta S(t)I(t) - (\mu + \gamma)E(t)\\
{}^{C}D_{*}^{\rho}I(t) &= \gamma E(t) - (\mu + \sigma + \alpha)I(t)\\
{}^{C}D_{*}^{\rho}R(t) &= \nu S(t) + \alpha I(t) - \mu R(t),
\end{aligned} \tag{19}$$

with initial conditions (11).

4. Stability Analysis

Herein, we aim to examine the primary properties of model (19) in view of various aspects including the invariant region, boundedness of solution, equilibrium point, BRN, and its elasticity.

4.1. The Invariant Region

This subsection intends to study the non-negativity of the solution of model (19). For instance, the solution of model (19) will be validated in accordance with the positive values of the initial conditions. For this purpose, we suppose for all non-negative values of t that the domain of the desired solution ψ has the following form:

$$\psi = \left\{ (S(t), E(t), I(t), R(t)) \in \mathbb{R}^4_+ : \ S(t) + E(t) + I(t) + R(t) \leq \frac{\Lambda}{\mu} \right\}, \tag{20}$$

where $S(t), E(t), I(t), R(t) \geq 0$. One could observe that all model parameters have non-negative values (i.e., $\sigma, \nu, \mu, \alpha, \gamma, \beta, \Lambda, \geq 0$). Now, in order to show the non-negativity of the solution of model (19), we recall the following two results, which would pave the way to achieve our first target.

Lemma 1 ([12,13]). *(Generalized Mean Value Theorem). Suppose that* $\Theta(t) \in C[a_1, a_2]$ *and* ${}^{C}D^{\rho}_{*}\Theta(t) \in C(a_1, a_2]$, *where* $0 < \rho \leq 1$, *then we have:*

$$\Theta(t) = \Theta(a_1) + \frac{1}{\Gamma(\rho)} \, {}^{C}D^{\rho}_{*}\Theta(\zeta)(t - a_1)^{\rho}, \tag{21}$$

where $0 \leq \zeta \leq t, \forall t \in (a_1, a_2]$.

Remark 1 ([12,13]). *Suppose that* $\Theta(t) \in C[0, \ a_2]$ *and* ${}^{C}D^{\rho}_{*}\Theta(t) \in C(0, \ a_2]$, *where* $0 < \rho \leq 1$. *In view of the above Lemma, one can conclude that, if* ${}^{C}D^{\rho}_{*}\Theta(t) \geq 0, \forall t \in (0, a_2]$, *then* $\Theta(t)$ *will be a non-decreasing vector-valued function, while if* ${}^{C}D^{\rho}_{*}\Theta(t) \leq 0, \forall t \in (0, a_2]$, *then such a function will be a non-increasing one.*

Theorem 2. *There exists a unique solution* $\Theta(t) = [S(t), E(t), I(t), R(t)]^T$ *of system (19), subject to the initial condition* $\Theta(0) = [S(0), E(0), I(0), R(0)]^T \in \mathbb{R}^4_+$, *and this solution will remain in* $\mathbb{R}^4_+$.

Proof. Tracking the necessary results deduced by the author in [13] leads us to identify, for definite, a unique solution $\Theta(t)$ on $(0, \infty)$ for system (19), subject to the initial condition $\Theta(0)$. On the other hand, in order to show that the domain $\mathbb{R}^4_+$ is indeed the positively invariant region, we have to observe the following assertions:

$$\begin{aligned}
&{}^{C}D^{\rho}_{*}S(t)|_{S=0} = (\Lambda - \beta S(t)I(t) - (\nu + \mu)S(t))|_{S=0} = \Lambda \geq 0,\\
&{}^{C}D^{\rho}_{*}E(t)|_{E=0} = (\beta S(t)I(t) - (\mu + \gamma)E(t))|_{E=0} = \beta S(t)I(t) \geq 0,\\
&{}^{C}D^{\rho}_{*}I(t)|_{I=0} = (\gamma E(t) - (\mu + \sigma + \alpha)I(t))|_{I=0} = \gamma E(t) \geq 0,\\
&{}^{C}D^{\rho}_{*}R(t)|_{R=0} = (\nu S(t) + \alpha I(t) - \mu R(t))|_{R=0} = \nu S(t) + \alpha I(t) \geq 0.
\end{aligned} \tag{22}$$

This validates that the solution of system (19) is non-negative over the domain given in (20). □

4.2. Boundedness of Solution

It was reported in [14] that the boundedness of the solution is regarded as a very important trait of this type of population model, with infectious diseases. In the epidemic population models, the solutions must be bounded, as unbounded solutions are physically meaningless. In what follows, we propose to show that the solution given at any specific

time for system (19) is bounded by $\frac{\Lambda}{\mu}$, as assumed previously in (20). For this purpose, we should note that

$$^{C}D_{*}^{\rho}N = {}^{C}D_{*}^{\rho}S + {}^{C}D_{*}^{\rho}E + {}^{C}D_{*}^{\rho}I + {}^{C}D_{*}^{\rho}R = \Lambda - \mu(S+E+I+R) - \sigma I,$$

where N is given in (12). Accordingly, we can have

$$^{C}D_{*}^{\rho}N = \Lambda - \mu N - \sigma I.$$

Under the assumed conditions in the domain ψ reported in (20), one could observe that $\sigma I \geq 0$, which yields the following inequality:

$$^{C}D_{*}^{\rho}N(t) \leq \Lambda - \mu N(t). \tag{23}$$

In order to solve the above inequality analytically with the initial conditions

$$N(0) = N_0, \tag{24}$$

we use the so-called Adomian decomposition method (or simply ADM), as it is very suitable in this case. To see this, we first operate I^{ρ} on both sides of the inequality (23) to obtain

$$N(t) \leq N_0 + I^{\rho}\Lambda - \mu I^{\rho}N(t),$$

or

$$N(t) \leq N_0 + \frac{\Lambda}{\Gamma(\rho+1)}t^{\rho} - \mu I^{\rho}N(t), \tag{25}$$

Now, in view of the ADM, the general solution of inequality (25) might be supposed as $N(t)=\sum_{k=0}^{\infty} N_k(t)$. This would immediately yield

$$\sum_{k=0}^{\infty} N_k(t) \leq N_0 + \frac{\Lambda}{\Gamma(\rho+1)}t^{\rho} - \mu I^{\rho}\left(\sum_{k=0}^{\infty} N_k(t)\right),$$

which consequently implies

$$\begin{aligned} N_0(t) &= N_0 + \frac{\Lambda}{\Gamma(\rho+1)}t^{\rho}, \\ N_k(t) &\leq -\mu I^{\rho}\left(\sum_{k=0}^{\infty} N_k(t)\right),\ k \geq 1. \end{aligned} \tag{26}$$

Thus, based on (26), we can obtain, for instance, $N_1(t)$ as follows:

$$N_1(t) \leq -\mu\left(\frac{N_0}{\Gamma(\rho+1)}t^{\rho} + \frac{\Lambda}{\Gamma(2\rho+1)}t^{2\rho}\right).$$

In the same way, we can obtain

$$N_2(t) \leq \mu^2\left(\frac{N_0}{\Gamma(2\rho+1)}t^{2\rho} + \frac{\Lambda}{\Gamma(3\rho+1)}t^{3\rho}\right).$$

If we continue in this manner, we obtain

$$N_3(t) \leq -\mu^3\left(\frac{N_0}{\Gamma(3\rho+1)}t^{3\rho} + \frac{\Lambda}{\Gamma(4\rho+1)}t^{4\rho}\right).$$

Now, due to the solution having the form $N(t) = \sum_{k=0}^{\infty} N_k(t)$, then, with the help of using the Mittag-Leffler function, we can gain

$$N(t) \leq \left(\frac{\Lambda}{\mu} - N_0\right) E_{\rho,1}(-\mu t^{\rho}). \tag{27}$$

Consequently, with the use of our assumptions in (20), we can deduce

$$N(t) \leq \frac{\Lambda}{\mu} - \left(\frac{\Lambda}{\mu} - N_0\right) E_{\rho,1}(-\mu t^{\rho}). \tag{28}$$

Therefore, the solution of system (19) is bounded by the term $\frac{\Lambda}{\mu}$ as $t \to \infty$, and hence this system is well-posed over its domain ψ.

4.3. The Disease-Free Equilibrium (DFE)

The DFE is the case in which society is clear of the Mpox illness. Such a point is $P_0 = (S_0, E_0, I_0, R_0)$, where $S_0 = S(0)$ is the initial susceptible state, $E_0 = E(0)$ is the initial exposed state, $I_0 = I(0)$ is the initial infected state, and $R_0 = R(0)$ is the initial recovered state. Thus, finding a solution for model (19), while considering $E_0 = 0$ and $I_0 = 0$, leads us to the following DFE:

$$P_0 = (S_0, E_0, I_0, R_0) = \left(\frac{\Lambda}{\mu + \nu}, 0, 0, \frac{\nu\Lambda}{\mu(\mu + \nu)}\right), \tag{29}$$

where $S_0 = \frac{\Lambda}{(\mu+\nu)}$ and $R_0 = \frac{\nu\Lambda}{\mu(\mu+\nu)}$.

4.4. The BRN R_0^*

The BRN is regarded a very significant index used to indicate the harshness of the infectious illness. It can be employed to describe the occurrence of the pandemic and the potential of outbreak. This index is regarded as an epidemiological measure to determine the hazard of the infectious transmission. With the aim of computing the BRN, we use the next-generation matrix method (NGMM), which was suggested in [15] and afterward developed in [16]. Such a method has been broadly employed for evaluating the BRN in a number of epidemiological models. Additionally, for the purpose of finding the BRN, we employ the NGMM by taking into account the exposed and infected classes. Afterward, we break down $\frac{dY}{dt} = Q - G$, in which $Q = \frac{dE}{dt}$ and $G = \frac{dI}{dt}$. This, consequently, gives

$$\frac{dY}{dt} = \begin{bmatrix} \frac{dE}{dt} \\ \frac{dI}{dt} \end{bmatrix}, \; Q = \begin{bmatrix} \beta S(t) I(t) \\ 0 \end{bmatrix}, \; G = \begin{bmatrix} (\mu + \gamma) E \\ -\gamma E + (\mu + \sigma + \alpha) I \end{bmatrix}. \tag{30}$$

Now, by computing the Jacobian matrices of Q and G at P_0 declared in (29), we obtain

$$\mathbb{G} = \begin{bmatrix} \gamma + \mu & 0 \\ -\gamma & \alpha + \mu + \sigma \end{bmatrix}, \; \mathbb{Q} = \begin{bmatrix} 0 & \frac{\beta\Lambda}{\mu+\nu} \\ 0 & 0 \end{bmatrix}. \tag{31}$$

Thus, we can evaluate R_0^* by finding the spectral radius $\Phi(\cdot)$ of the (NGMM) $\mathbb{F} = \mathbb{Q}\mathbb{G}^{-1}$. In other words, we have

$$R_0^* = \Phi(\mathbb{F}) = \Phi(\mathbb{Q}\mathbb{G}^{-1}) = \frac{\beta\gamma\Lambda}{(\gamma + \mu)(\mu + \nu)(\alpha + \mu + \sigma)}. \tag{32}$$

4.5. Local Sensitivity and Elasticity Analysis of R_0^*

In the field of epidemiological models, the parameters' values have a vital role in computing R_0^*. Under the assumption that all parameters are retained at specific values (estimated) including the parameter ϱ, we call this measure "local sensitivity" [17]. In such

a measure, the formula used to evaluate the effect of changing one parameter ϱ on R_0^* is written as

$$S_{\varrho}^{R_0^*} = \frac{\partial R_0^*}{\partial \varrho}. \tag{33}$$

However, although this method does not consider a simultaneous changing of all parameters, it is influenced highly by the values of ϱ and R_0^*. Hence, a better indicator will be the elasticity which is defined by the change in the quantity of R_0^*, as a percentage, due to the value change of the parameter ϱ, as a percentage. The formula of elasticity is written as

$$\Upsilon_{\varrho}^{R_0^*} = \left(\frac{\partial R_0^*}{\partial \varrho}\right)\left(\frac{\varrho}{R_0^*}\right) \approx \mp \frac{\%\Delta R_0^*}{\%\Delta \varrho}, \tag{34}$$

where a positive elasticity indicates an increment in R_0^* in terms of the parameter ϱ, while a negative elasticity indicates a decrement in R_0^*, in terms of the parameter ϱ.

From Equation (32) of R_0^* and using the elasticity Equation (34), we investigate the elasticity for all parameters of the model. From this point of view, we can calculate the local elasticity of R_0^* in relation to the vaccination rate (ν) as

$$\Upsilon_{\nu}^{R_0^*} = \left(\frac{\partial R_0^*}{\partial \nu}\right)\left(\frac{\nu}{R_0^*}\right) = \frac{\beta\gamma\Lambda}{(\gamma+\mu)(\mu+\nu)^2(\alpha+\mu+\sigma)}\left(\frac{\nu}{R_0^*}\right) = -\frac{\nu}{\mu+\nu} < 0. \tag{35}$$

Since the value of ν indicates the vaccination rate, then the increment of this rate leads to the decrement of R_0^* and, thus, negatively affects the spreading of the disease. To see this, we plot Figure 2 based on the data reported in Table 2. This figure clearly shows the influence of the vaccination rate v on R_0^* and, hence, confirms our aforesaid claim.

Table 2. The parameters of the fractional-order Mpox model.

Parameter	Value
Λ	163/10,000
β	0.5
γ	0.05
α	1/17
μ	91/10,000
ν	Changes within $[0, 1]$
σ	0.03

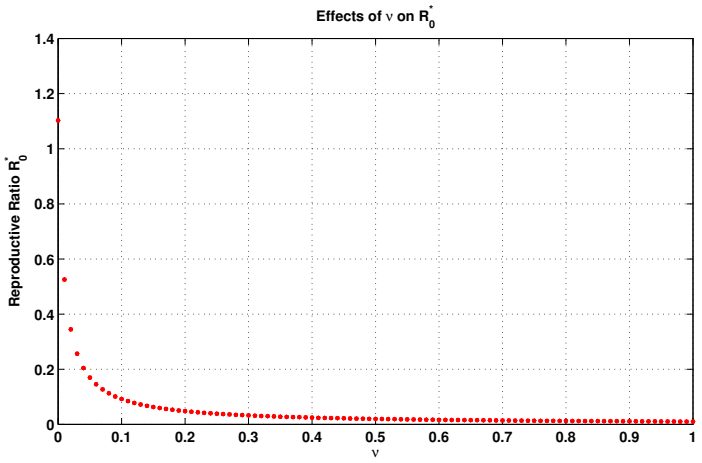

Figure 2. Influence of the vaccination rate v on R_0^*.

On the other hand, the local elasticity of R_0^*, in relation to the contact transmission rate (β), can be computed as

$$\Upsilon_{\beta}^{R_0^*} = \left(\frac{\partial R_0^*}{\partial \beta}\right)\left(\frac{\beta}{R_0^*}\right) = \frac{\gamma\Lambda}{(\gamma+\mu)(\mu+\nu)(\alpha+\mu+\sigma)}\left(\frac{\beta}{R_0^*}\right) = 1 > 0. \tag{36}$$

Thus,the increment of the transmission rate β by 1% leads to a rise in R_0^*. This is the case of spreading infectious diseases due to the increment in personal contact and communications between individuals and due to the pathogen specifications. However, we plot Figure 3 on the basis of the same values reported in Table 2, but here we take $\nu = 0.15$ and allow β to be varied from 0.045 to 0.18. Such a figure also shows the influence of the transmission rate β on R_0^*, which completely coincides with our algebraic calculations mentioned previously.

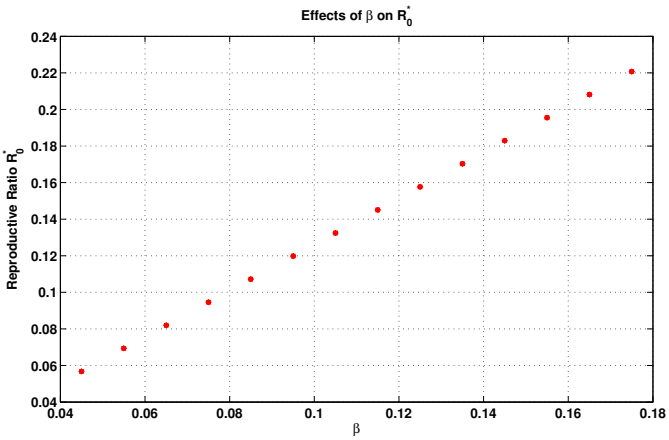

Figure 3. Influence of the transmission rate β on R_0^*.

In the same manner, the local elasticity of R_0^*, in relation to the transmission rate (α) from the I state to the R state, can be computed as

$$\Upsilon_{\alpha}^{R_0^*} = \left(\frac{\partial R_0^*}{\partial \alpha}\right)\left(\frac{\alpha}{R_0^*}\right) = \frac{\beta\gamma\Lambda}{(\gamma+\mu)(\mu+\nu)(\alpha+\mu+\sigma)^2}\left(\frac{\alpha}{R_0^*}\right) = -\frac{\alpha}{\alpha+\mu+\sigma} < 0. \tag{37}$$

The inversevalue of α, which is α^{-1}, is the recovery period. So, the increment in α (decrement in recovery period) leads to a decrement in R_0^*. This reflects the movement rate rise from the I state to the R state, and, consequently, the individuals become immunized. This would negatively affect the spreading of disease. Now, by taking $\nu = 0.15$ and $\beta = 0.05$, and by keeping the remaining parameters as they are in Table 2, except for changing α within the interval $\left[\frac{1}{32}, \frac{1}{15}\right]$, we plot Figure 4, which shows the influence of the transmission rate α on R_0^* as well. This also confirms our assertion discussed previously.

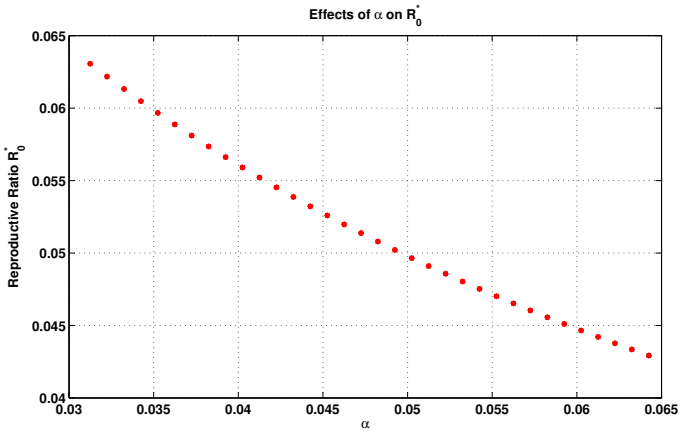

Figure 4. Influence of the transmission rate α on R_0^*.

It should be mentioned here, that based on the data reported in Table 2, we can easily compute the BRN as $R_0^* = 0.000611$, and due to this value being less than 1, then one can deduce that the Mpox illness will not promptly spread.

5. Numerical Findings

In the following content, we intend to employ two numerical methods (the FEM and MFEM) to obtain approximate solutions of the fractional-order Mpox system (19). In fact, these methods represent two fractional versions of the conventional Euler method. One can refer to [8] for the purpose of obtaining a comprehensive view about such methods. In this context, Theorem 1 can lay the foundation to recall the FEM and MFEM, which are considered for the following fractional problem:

$$ {}^{C}D_{*}^{\rho} z(x) = g(t, z(t)),\ z(0) = z_0,\ t > 0,\ 0 < \rho \leq 1. \tag{38} $$

To address problem (38), we assume $[0, a]$ as the interval over which we wish to obtain the desired numerical solution. In general, we are not capable to find $z(t)$, which represents the analytical solution to the problem at hand. As an alternative, we can establish a set of points $(t_i, z(t_i))$, and then employ them in finding the approximate solution [8,18]. For simplification purposes, we divide $[0, a]$ into k sub-intervals $[t_i, t_{i+1}]$ with $h = a/k$ through $t_i = ih$, for $i = 0, 1, 2, \ldots, k$. Now, we assume that $z(t)$, ${}^{C}D_{*}^{\rho} z(t)$, and ${}^{C}D_{*}^{2\rho} z(t)$ are continuous on $(0, a]$. Therefore, by means of Theorem 1, one might expand $z(t)$ about $t = t_i$ as

$$ z(t) = z(t_i) + \frac{(t - t_i)^{\rho}}{\Gamma(\rho + 1)} {}^{C}D_{*}^{\rho} z(t_i) + \frac{(t - t_i)^{2\rho}}{\Gamma(2\rho + 1)} {}^{C}D_{*}^{2\rho} z(\xi), \tag{39} $$

for some $\xi \in (t_i, t_{i+1})$. Thus, if we substitute t_{i+1} instead of t in (39), we obtain

$$ z(t_{i+1}) = z(t_i) + \frac{h^{\rho}}{\Gamma(\rho + 1)} {}^{C}D_{*}^{\rho} z(t_i) + \frac{(t_{i+1} - t_i)^{2\rho}}{\Gamma(2\rho + 1)} {}^{C}D_{*}^{2\rho} z(\xi), \tag{40} $$

for some $\xi \in (t_i, t_{i+1})$. Now, if one chooses $h = t_{i+1} - t_i$ too small, then the last term of (40) can be eliminated to obtain

$$ z(t_{i+1}) = z(t_i) + \frac{h^{\rho}}{\Gamma(\rho + 1)} {}^{C}D_{*}^{\rho} z(t_i). \tag{41} $$

Actually, Equation (41) represents the primary formula of the FEM. In the same regard, if one substitutes

$$ {}^{C}D_{*}^{\rho} z(t_{i+1}) = g\left(t_i + \frac{h^{\rho}}{\Gamma(\rho + 1)}, z(t_i) + \frac{h^{\rho}}{\Gamma(\rho + 1)} g(t_i, z(t_i))\right) $$

instead of (41), the result of $z(t_{i+1})$ will be consequently yielded. In other words, we obtain

$$ z(t_{i+1}) = z(t_i) + \frac{h^{\rho}}{\Gamma(\rho + 1)} \times g\left(t_i + \frac{h^{\rho}}{\Gamma(\rho + 1)}, z(t_i) + \frac{h^{\rho}}{\Gamma(\rho + 1)} g(t_i, z(t_i))\right), \tag{42} $$

for $i = 0, 1, 2, \ldots, k - 1$. Equation (42) represents the main formula of the MFEM that would be compared next with the FEM's formula. In what follows, we attempt to implement only the MFEM on the fractional-order Mpox system (19), as the FEM is similar to the MFEM. To do so, we reconsider such a system again as

$$ \begin{aligned} {}^{C}D_{*}^{\rho} S(t) &= g_1(t, S(t), E(t), I(t), R(t)) \\ {}^{C}D_{*}^{\rho} E(t) &= g_2(t, S(t), E(t), I(t), R(t)) \\ {}^{C}D_{*}^{\rho} I(t) &= g_3(t, S(t), E(t), I(t), R(t)) \\ {}^{C}D_{*}^{\rho} R(t) &= g_4(t, S(t), E(t), I(t), R(t)), \end{aligned} \tag{43} $$

where

$$\begin{aligned} g_1(t, S(t), E(t), I(t), R(t)) &= \Lambda - \beta S(t)I(t) - (\nu + \mu)S(t) \\ g_2(t, S(t), E(t), I(t), R(t)) &= \beta S(t)I(t) - (\mu + \gamma)E(t) \\ g_3(t, S(t), E(t), I(t), R(t)) &= \gamma E(t) - (\mu + \sigma + \alpha)I(t) \\ g_4(t, S(t), E(t), I(t), R(t)) &= \nu S(t) + \alpha I(t) - \mu R(t). \end{aligned} \tag{44}$$

More precisely, with the aim of generating $(t_k, S(t_k))$ in relation to the compartment S, one should suppose that $S(t)$, ${}^{C}D^{\rho}_{*}S(t)$, and ${}^{C}D^{2\rho}_{*}S(t)$ are all continuous on $(0, T]$. From this perspective, if we assume that

$$g_1(t, S(t), E(t), I(t), R(t)) = \Lambda - \beta S(t)I(t) - (\nu + \mu)S(t),$$

so that

$${}^{C}D^{\rho}_{*}S(t) = g_1(t, S(t), E(t), I(t), R(t)),$$

then, with the use of (42), one might obtain

$$S(t_{i+1}) = S(t_i) + \frac{h^{\rho}}{\Gamma(\rho+1)} \times g_1\left(t_i + \frac{h^{\rho}}{\Gamma(\rho+1)}, S(t_i) + \frac{h^{\rho}}{\Gamma(\rho+1)} g_1(t_i, S(t_i))\right), \tag{45}$$

for $i = 0, 1, 2, \ldots, k-1$.

In a similar manner, the aforesaid approach might be applied for the remaining classes to obtain their approximate solutions. In the long run, we can infer the following approximations of model (19):

$$\begin{aligned} S(t_{i+1}) &= S(t_i) + \frac{h^{\rho}}{\Gamma(\rho+1)} \times g_1\left(t_i + \frac{h^{\rho}}{\Gamma(\rho+1)}, S(t_i) + \frac{h^{\rho}}{\Gamma(\rho+1)} g_1(t_i, S(t_i))\right), \\ E(t_{i+1}) &= E(t_i) + \frac{h^{\rho}}{\Gamma(\rho+1)} \times g_2\left(t_i + \frac{h^{\rho}}{\Gamma(\rho+1)}, E(t_i) + \frac{h^{\rho}}{\Gamma(\rho+1)} g_2(t_i, E(t_i))\right), \\ I(t_{i+1}) &= I(t_i) + \frac{h^{\rho}}{\Gamma(\rho+1)} \times g_3\left(t_i + \frac{h^{\rho}}{\Gamma(\rho+1)}, I(t_i) + \frac{h^{\rho}}{\Gamma(\rho+1)} g_3(t_i, I(t_i))\right), \\ R(t_{i+1}) &= R(t_i) + \frac{h^{\rho}}{\Gamma(\rho+1)} \times g_4\left(t_i + \frac{h^{\rho}}{\Gamma(\rho+1)}, R(t_i) + \frac{h^{\rho}}{\Gamma(\rho+1)} g_4(t_i, R(t_i))\right), \end{aligned} \tag{46}$$

where g_1, g_2, g_3, g_4 are already outlined in (44), $i = 0, 1, 2, \ldots, k-1$.

In the following content, we propose to depict certain numerical findings that demonstrate the dynamics of the fractional-order Mpox system (19). In this connection, we consider Table 3, which takes very close data to certain available data captured out of the Indian community, on the basis of reference [19,20].

Table 3. Parameters of system (19) [19].

Parameter	Value
$S(0)$	23
$E(0)$	6
$I(0)$	4
$R(0)$	0
Λ	0.01630
β	0.05000
γ	0.05882
α	0.03125
μ	0.00910
ν	$[0, 1]$
σ	0.0300

On the basis of the previous discussion, we compare, in Figures 5–8, between several MFEMs' solutions for the I and E of system (19), in accordance with several fractional-order values of ρ. The primary goal of these simulations is to notice the impact of the vaccination rate on the exposed and infected states.

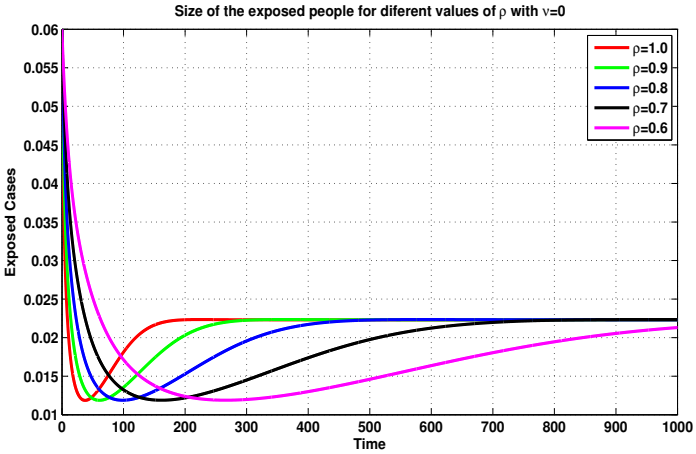

Figure 5. Exposed sizes $E \times 10^2$ of system (19) for $\rho = 1, 0.9, 0.8, 0.7, 0.6$ through MFEM with $\nu = 0$.

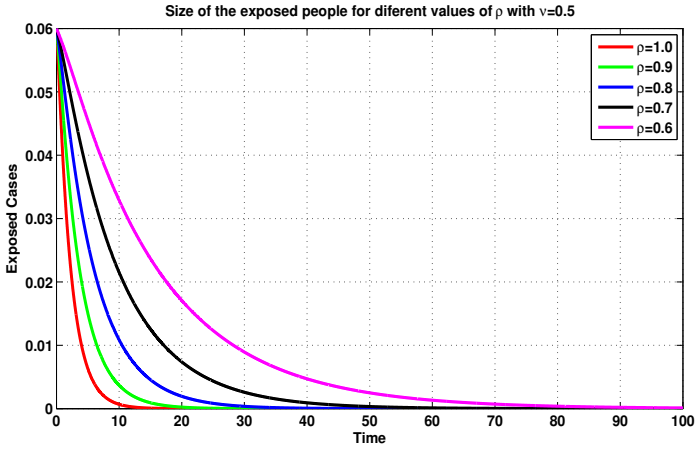

Figure 6. Exposed sizes $E \times 10^2$ of system (19) for $\rho = 1, 0.9, 0.8, 0.7, 0.6$ through MFEM with $\nu = 0.5$.

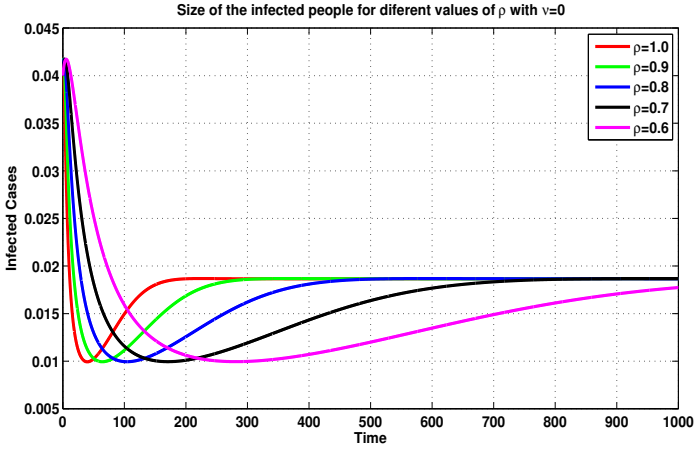

Figure 7. Infected sizes $I \times 10^2$ of system (19) for $\rho = 1, 0.9, 0.8, 0.7, 0.6$ through MFEM with $\nu = 0$.

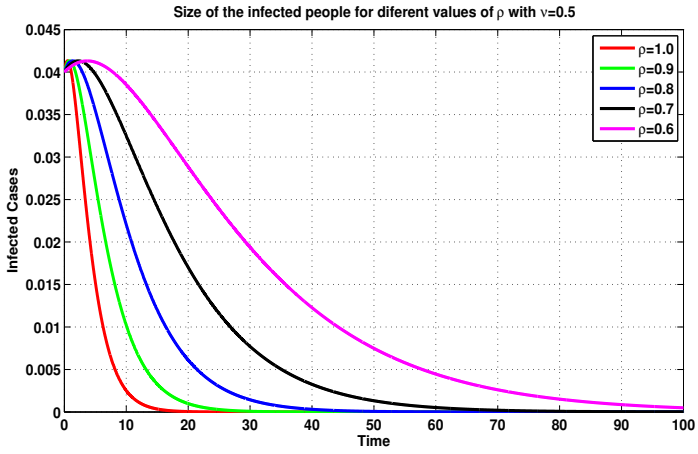

Figure 8. Infected sizes $I \times 10^2$ of system (19) for $\rho = 1, 0.9, 0.8, 0.7, 0.6$ through MFEM with $\nu = 0.5$.

For further description and in accordance with $\rho = 0.75$, we simulate, once again, the infected and exposed sizes of system (19), as shown in Figures 9 and 10, by using the MFEM with and without consideration of the vaccination rate ν. Accordingly, one might obviously notice that, if the vaccination rate is raised, then the amounts of the exposed and infected states are reduced, validating the impact of such a rate on the model at hand.

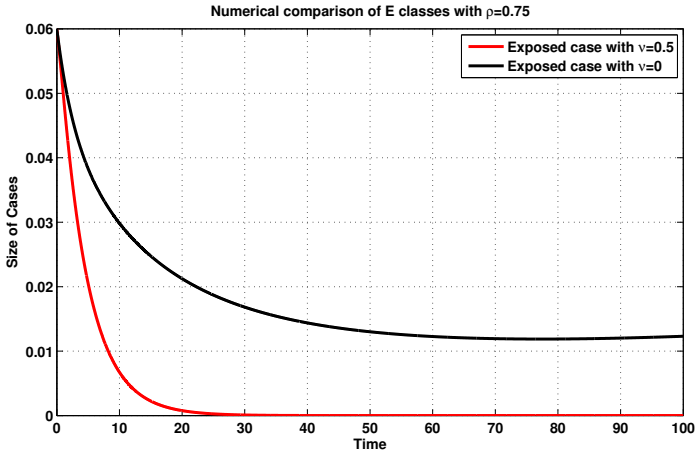

Figure 9. Exposed sizes $E \times 10^2$ of system (19) for $\rho = 0.75$ with and without considering ν.

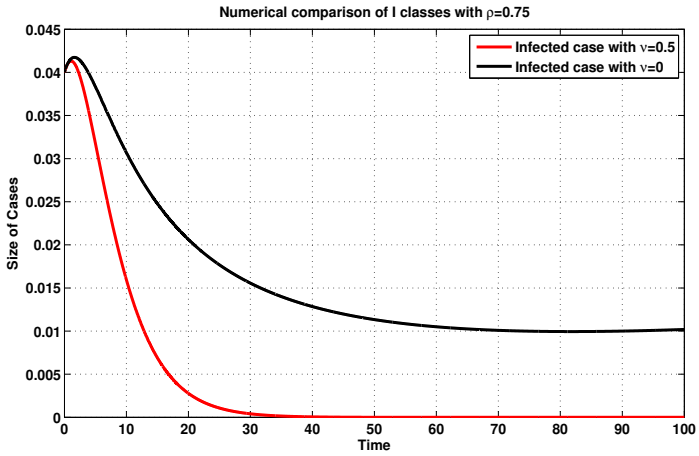

Figure 10. Infected sizes $I \times 10^2$ of system (19) for $\rho = 0.75$ with and without considering ν.

For the same connection, it was demonstrated in [8] that the MFEM is a modified numerical scheme for the FEM. Thus, with the aim of validating the numerical results

generated by using the MFEM, we make some comparisons between its numerical results and the FEM's numerical results (see Figures 11–14).

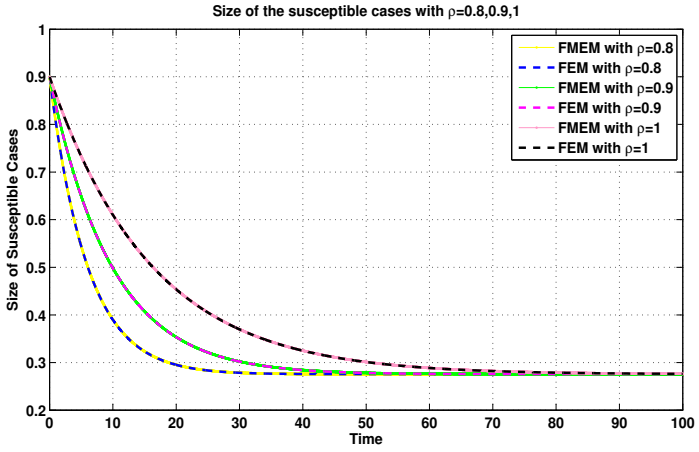

Figure 11. Susceptible sizes $S \times 10^2$ of system (19) for $\rho = 0.6, 0.7, 0.8, 0.9, 1$ using FEM and MFEM.

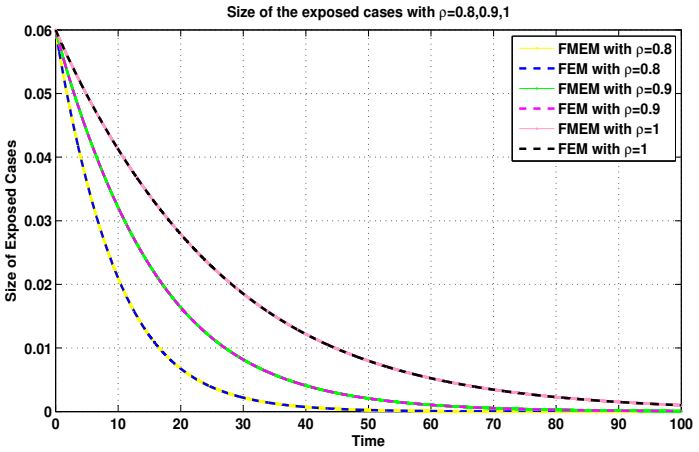

Figure 12. Exposed sizes $E \times 10^2$ of system (19) for $\rho = 0.6, 0.7, 0.8, 0.9, 1$ using FEM and MFEM.

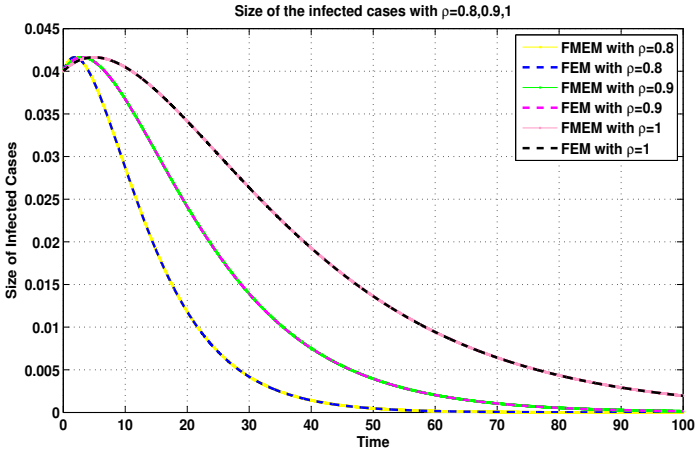

Figure 13. Infected sizes $I \times 10^2$ of system (19) for $\rho = 0.6, 0.7, 0.8, 0.9, 1$ using FEM and MFEM.

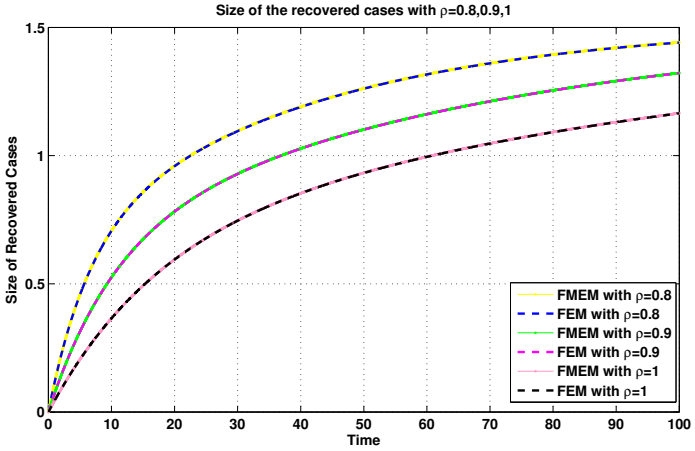

Figure 14. Recovered sizes $R \times 10^2$ of system (19) for $\rho = 0.6, 0.7, 0.8, 0.9, 1$ using FEM and MFEM.

In the same regard, for the purpose of showing the validity of the domain ψ reported in Section 4.1 and the validity of the boundedness of solution of system (19) discussed in Section 4.2, one can easily check, based on the data reported in Table 3, that the sum of all classes satisfies the inequality declared in (20). In other words, one can check

$$S(t) + E(t) + I(t) + R(t) \leq 1.79121. \tag{47}$$

This bound is further confirmed numerically by plotting the sum of $S(t) + E(t) + I(t) + R(t)$ according to different fractional-order values, as shown in Figure 15.

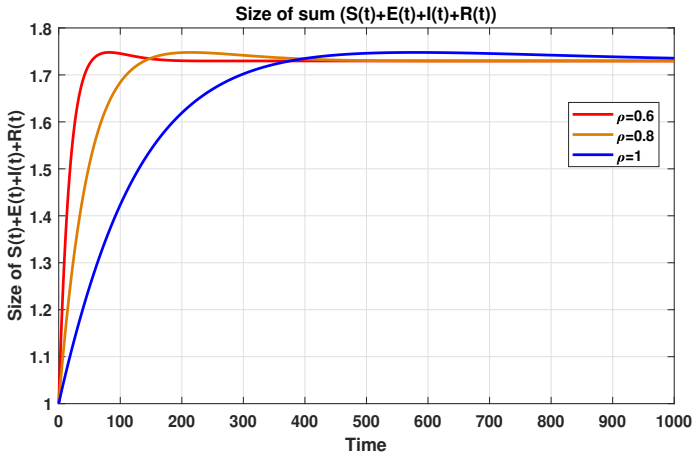

Figure 15. The sizes of $S(t) + E(t) + I(t) + R(t)$ for $\rho = 0.6, 0.8, 1$ using MFEM.

6. Conclusions

In this study, a novel fractional-order version of Mpox disease has been established in light of the Caputo operator. Accordingly, several innovative findings connecting to the stability analysis have been addressed. In the same connection, the proposed Mpox model has been numerically solved with the use of the FEM and MFEM. As a consequence of concentrating on the numerical findings, we can obviously notice that the behavior of the proposed fractional-order Mpox model is affected by performing any variation in the value of the fractional-order. This enables us to gain more extra degrees of freedom for the established model. In addition, we observe that the behavior of the MFEM's solutions is completely coincided with the FEM's ones, confirming the validity of the computational methods used in this work. Based on these solutions, it can be clearly concluded that, if the rate of vaccination is raised, then the exposed and infectious sizes are reduced gradually, confirming the influence of this rate. More precisely, if the vaccination aspect is regarded,

then the infectious and exposed cases will vanish in the long run. This will consequently cause Mpox illness to be under control eventually.

Author Contributions: Conceptualization, I.M.B. and I.H.J.; methodology, A.A.A. and M.A.; software, S.B.A.-S.; validation, K.M.; formal analysis, I.M.B.; investigation, A.A.A. and M.A.; resources, S.B.A.-S.; data curation, I.H.J.; writing—original draft preparation, K.M.; writing—review and editing, I.M.B.; visualization, A.A.A. and M.A.; supervision, I.H.J.; project administration, S.B.A.-S.; funding acquisition, K.M. All authors have read and agreed to the published version of the manuscript.

Funding: The authors extend their appreciation to Arab Open University for funding this research through AOU research fund No. AOURG-2023-008.

Data Availability Statement: Not applicable.

Acknowledgments: The authors would like to thank the Arab Open University and Al-Zaytoonah University for providing the necessary scientific research supplies to implement the research.

Conflicts of Interest: The authors declare no conflict of interest.

References

1. Suvvari, T.K.; Ghosh, A.; Lopinti, A.; Islam, M.A.; Bhattacharya, P. Hematological manifestations of Monkeypox virus (MPOX) and impact of human MPOX disease on blood donation—What we need to know? *New Microbes New Infect.* **2023**, *52*, 101108. [CrossRef] [PubMed]
2. Adetifa, I.; Muyembe, J.-J.; Bausch, D.G.; Heymann, D.L. Mpox neglect and the smallpox niche: A problem for Africa, a problem for the world. *Lancet* **2023**, *401*, 1822–1824. [CrossRef]
3. Sam-Agudu, N.A.; Martyn-Dickens, C.; Ewa, A.U. A global update of mpox (monkeypox) in children. *Curr. Opin. Pediatr.* **2023**, *35*, 193–200. [CrossRef] [PubMed]
4. Jahanshahi, H.; Munoz-Pacheco, J.M.; Bekiros, S.; Alotaibi, N.D. A fractional-order SIRD model with time-dependent memory indexes for encompassing the multi-fractional characteristics of the COVID-19. *Chaos Solitons Fractals* **2021**, *143*, 110632. [CrossRef] [PubMed]
5. Stuart, C.I.J.M.; Takahashi, Y.; Umezawa, H. On the stability and non-local properties of memory. *J. Theor. Biol.* **1978**, *71*, 605–618. [CrossRef]
6. Peter, O.J.; Oguntolu, F.A.; Ojo, M.M.; Oyeniyi, A.O.; Jan, R.; Khan, I. Fractional order mathematical model of monkeypox transmission dynamics. *Phys. Scr.* **2022**, *97*, 084005. [CrossRef]
7. Rexma Sherine, V.; Chellamani, P.; Ismail, R.; Avinash, N.; Xavier, G.B.A. Estimating the Spread of Generalized Compartmental Model of Monkeypox Virus Using a Fuzzy Fractional Laplace Transform Method. *Symmetry* **2022**, *14*, 2545. [CrossRef]
8. Batiha, I.M.; Bataihah, A.; Al-Nana, A.A.; Alshorm, S.; Jebril, I.H.; Zraiqat, A. A numerical scheme for dealing with fractional initial value problem. *Int. J. Innov. Comput. Inf. Control* **2023**, *19*, 763–774. [CrossRef]
9. Kilbas, A.A. *Theory and Application of Fractional Differential Equations*; Elsevier: Amsterdam, The Netherlands, 2006.
10. Almuzini, M.; Batiha, I.M.; Momani, S. A study of fractional-order monkeypox mathematical model with its stability analysis. In Proceedings of the 2023 International Conference on Fractional Differentiation and Its Applications (ICFDA), Ajman, United Arab Emirates, 14–16 March 2023; pp. 1–6. [CrossRef]
11. Garba, S.M.; Gumel, A.B.; Lubuma, J.M.-S. Dynamically-consistent non-standard finite difference method for an epidemic model. *Math. Comput. Model.* **2011**, *53*, 131–150. [CrossRef]
12. Lin, W. Global existence theory and chaos control of fractional differential equations. *J. Math. Anal. Appl.* **2007**, *332*, 709–726. [CrossRef]
13. Naik, P.A.; Zu, J.; Owolabi, K.M. Global dynamics of a fractional order model for the transmission of HIV epidemic with optimal control. *Chaos Solitons Fractals* **2020**, *138*, 109826. [CrossRef] [PubMed]
14. Iqbal, Z.; Ahmed, N.; Baleanu, D.; Adel, W.; Rafiq, M.; Aziz-ur Rehman, M.; Alshomrani, A.S. Positivity and boundedness preserving numerical algorithm for the solution of fractional nonlinear epidemic model of HIV/AIDS transmission. *Chaos Solitons Fractals* **2020**, *134*, 109706. [CrossRef]
15. Diekmann, O.; Heesterbeek, J.A.P.; Metz, J.A. On the definition and the computation of the basic reproduction ratio R0 in models for infectious diseases in heterogeneous populations. *J. Math. Biol.* **1990**, *28*, 365–382. [CrossRef] [PubMed]
16. Van den Driessche, P.; Watmough, J. Reproduction numbers and sub-threshold endemic equilibria for compartmental models of disease transmission. *Math. Biosci.* **2002**, *180*, 29–48. [CrossRef] [PubMed]
17. Morio, J. Global and local sensitivity analysis methods for a physical system. *Eur. J. Phys.* **2011**, *32*, 1577. [CrossRef]
18. Zraiqat, A.; Paikrayb, S.K.; Duttac, H. A Certain Class of Deferred Weighted Statistical B-Summability Involving (p,q)-Integers and Analogous Approximation Theorems. *Filomat* **2019**, *33*, 1425–1444.

19. Statisticstimes.com. Countries by GDP Growth. 2020. Available online: https://statisticstimes.com (accessed on 15 March 2023).
20. van den Driessche, P. Reproduction numbers of infectious disease models. *Infect. Dis. Model.* **2017**, *2*, 288–303. [PubMed]